

## **$\mu$ -Synthesis robust control of double-effect distillation columns**

MANSOUR A. KARKOUB

*Mechanical Engineering Department, College of Engineering and Petroleum, Kuwait University, Tel: +965 481 7381, Fax: +965 484 7131. e-mail: mansourk@kuc01.kuniv.edu.kw*

### **ABSTRACT**

The control of double-effect distillation columns has been the subject of a great deal of research for the past few years. The preferred control tool used for distillation columns is the Proportional Plus Integral (PI). However, this technique requires a fairly accurate model and does not guarantee robust performance in the presence of modeling and other errors. Therefore, a control design technique that will account for the shortcomings of the dynamic model has to be used. The  $\mu$ -synthesis technique has been proven to be a good tool to bridge the gap between the modeling and control design processes. Two controllers are designed for a double-effect distillation column using the  $\mu$ -synthesis control design technique. The controllers are designed for the model derived by Al-Elg and Palazoglu (1989). The resultant work leads to a much better response for the HP and LP distillates as well as the LP and HP bottoms. Moreover, the designed controllers are robust to variations in the high frequency dynamics, actuation and input uncertainties, and noise.

**Keywords:** Double effect distillation columns;  $\mu$ -synthesis; robust control.

### **INTRODUCTION**

The subject of modeling and control of distillation columns has been studied extensively for the past two decades. Many publications are available in the literature; however, only a representative few will be discussed here. One model for distillation columns that is readily available in the literature is that of Skogestad and Morari (1988), who developed a model for a high purity distillation column. The modeling technique used a logarithmic representation which led to a simple linear model. This technique was used by many other authors, such as Han and Park (1996). The use of this technique minimizes the effect of nonlinearities and high frequency dynamics of the system. Lee and Morari (1990) have used a simplified model for distillation columns for control purposes. The model is obtained empirically and does not account for the inherent time delays of the system. Al-Elg and Palazoglu (1989) derived a dynamic model for a high purity double-effect distillation column. The model was derived theoretically based on many assumptions such as 100% efficiency and no transport lag. The authors designed PI controllers for the system using the biggest log modulus analysis. The results of the control action

are discussed in this paper. Han and Park (1996) derived a model for a double-effect distillation column; they assumed both columns to have 20 trays and the feeds were introduced at the 16th and 11th tray respectively. The authors also assumed negligible pressure drop between trays, ideal vapor-liquid equilibrium, and the tray efficiency to be 100%.

Several control techniques have been used to control distillation columns, the most common of which is PI control. Skogestad and Morari (1988) designed PI controllers and utilized structured uncertainty analysis to check the robustness of the controllers. Al-Elg and Palazoglu (1989) derived two PI controllers based on Ziegler-Nichols and the largest modulus methods. The controllers performed well for the prescribed conditions. Han and Park (1996) took a slightly different approach to the control of double-effect distillation columns in which they designed a model-based control scheme. The shortcoming of this work is that the control is essentially obtained by inverting the system.

The control design models discussed in the previous paragraphs are derived based on certain assumptions as well as practical simplifications. These simplifications lead to relatively inaccurate models, especially at high frequencies. Consequently, this puts a limitation on the bandwidth of the designed controllers. One other aspect that is not considered in most available models is the fact that all parameters of the system are considered constant. However, it is well known that certain parameters are dynamic and change with time and temperature. Small as they may be, these changes can have an effect on the overall behavior of the system. The  $H_\infty$  design technique assumes that the model might have a finite amount of uncertainty related to the parameters and other inputs. This modeling scheme allows us to incorporate the shortcomings of the control design model into the control design process, thus bridging the gap between the modeling and control design processes.

In this paper, the  $\mu$ -synthesis technique, which is an extension of the  $H_\infty$  control design tool, is used to derive a control law for a double-effect distillation column. the dynamic model (transfer matrix) of the column is derived by Al-Elg and Palazoglu (1989) and it is given by:

$$T(s) = \begin{bmatrix} \frac{-2.62e^{-0.02s}}{2.907s + 1} & \frac{1.375e^{-0.06s}}{3.075s + 1} & \frac{-1.265e^{-0.02s}}{2.907s + 1} & 0 \\ \frac{-1.895e^{-0.96s}}{4.834s + 1} & \frac{1.285e^{-0.014s}}{3.835s + 1} & \frac{-1.095e^{-0.202s}}{3.835s + 1} & 0 \\ 0 & 0 & \frac{0.75e^{-0.03s}}{3.185s + 1} & \frac{0.53e^{-0.058s}}{3.027s + 1} \\ 0 & 0 & \frac{0.71e^{-0.53s}}{2.41s + 1} & \frac{0.53e^{-0.058s}}{3.027s + 1} \end{bmatrix}. \quad (1)$$

The time delays in the transfer functions are obtained empirically.

The rest of the paper is organized as follows: the  $\mu$ -synthesis control technique as well as the "D-K" iteration procedure are explained in Section 2. A comparison between the proposed control scheme, PI control, and the inverse based control

technique is also given in Section 2. The  $\mu$ -synthesis controller design is discussed in Section 3. The simulation results are presented in Section 4. Finally, some concluding remarks are given in Section 5.

### THE $\mu$ -SYNTHESIS CONTROL TECHNIQUE

The  $\mu$ -synthesis technique (Doyle 1982, Balas *et al.* 1991, Karkoub *et al.* 2000) will be used in this paper to design robust controllers for distillation columns. A detailed explanation of this technique ( $\mu$ -synthesis) is provided in this section. The control strategy is discussed first to better understand what must be achieved to meet performance and stability objectives.

Most models found in the literature do not actually represent distillation columns accurately because:

- Noise is not accounted for;
- Uncertainty of system parameters is not directly taken into account;
- Certain phenomena are not accounted for; and
- Simplifying assumptions are made.

Some of these sources of error must be accounted for in the control design. The rest of the section provides a general idea on how this can be accomplished.

Let us assume that a plant,  $G_0$ , to be controlled, has some dynamics that need to be accounted for. The plant can be represented as follows:

$$G = G_0 + \Delta_a \tag{2}$$

where  $G_0$  is the nominal plant. Restricting our attention to bounded uncertainty (Maciejowski 1989), weighting functions can be selected such that:

$$\|\Delta_a\|_\infty \leq 1. \tag{3}$$

Equation (2)

$$G = G_0 + W_1 \Delta_a W_2 \tag{4}$$

where  $W_1$  and  $W_2$  are stable, minimum phase transfer functions that capture the magnitude and direction of the uncertainty. The nominal plant may be obtained by setting  $\Delta_a$  to zero.

Any controller designed for the kind of plants described by Eq. (2), has to stabilize not only the nominal plant, but also all the plants generated by the addition of uncertainty. For this controller to exist, one has to develop some kind of a condition that guarantees robust stability.

Let us consider a nominal plant  $G_0$  with an additive uncertainty (see Fig. 1). It can be easily shown that the control system can be rearranged to look like the one in Fig. 2 where the elements of  $P$  are defined in Eqs. (5) through (8).

$$P_{11} = G_0K(I + G_0K)^{-1} \tag{5}$$

$$P_{12} = (I + G_0K)^{-1}W_1 \tag{6}$$

$$P_{21} = W_2(I + G_0K)^{-1}K \tag{7}$$

$$P_{22} = -W_2(I + G_0K)^{-1}KW_1 \tag{8}$$

where  $K$  is the stabilizing controller for the nominal plant  $G_0$ .

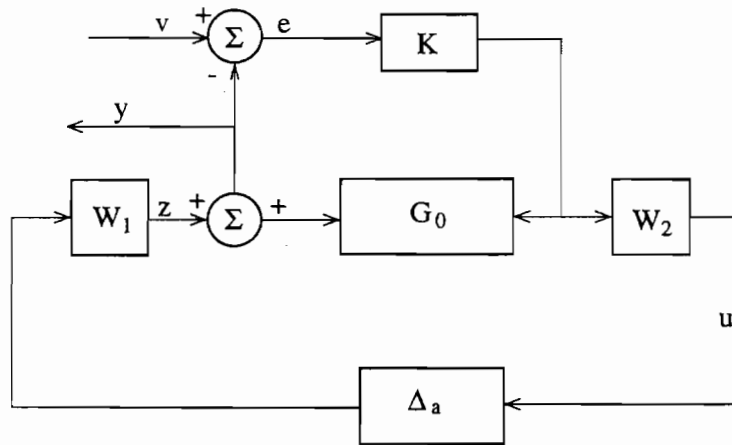


**Fig. 1.** Block diagram of a system with additive uncertainty.

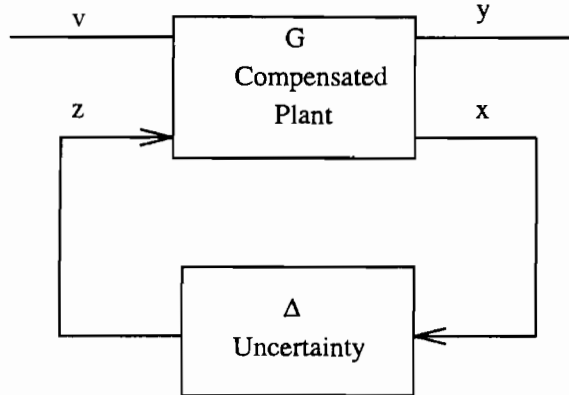


**Fig. 2.** Block diagram of the compensated plant.

It can be shown that for the feedback system to be stable for all stable bounded uncertainty  $\Delta_a$ , the infinity norm of  $P_{22}$  had to be less than 1. In other words, to achieve robust stability the following condition has to be met:

$$\|P_{22}\|_\infty \leq 1. \tag{9}$$

This condition for robust stability was derived with no consideration for the nature of the uncertainty; i.e., the uncertainty matrix  $\Delta$  in Fig. 2 is a fully populated matrix. However, if we consider the case where  $\Delta$  is block diagonal with each block  $\Delta_j$  having an infinity norm less than 1 ( $\|\Delta_j\|_\infty \leq 1$ ), the condition described by Eq. (9) becomes conservative. (The condition  $\|P_{22}\|_\infty \leq 1$  is still valid even for the structured case; however, it is no longer a necessary condition.) Therefore, the condition for robust stability has to be revised for the structured uncertainty case.

There are two types of uncertainty blocks: repeated-scalar and full blocks.

Let  $\Delta$  in  $C^{n \times n}$  be defined as follows:

$$\Delta = \left\{ \begin{array}{l} \text{diag}[\delta_1 I_{r_1}, \dots, \delta_s I_{r_s}, \Delta_1, \dots, \Delta_F] \\ \delta_i \in C, \Delta_j \in C^{m_j \times m_j} \end{array} \right\} \tag{10}$$

and

$$B\Delta = \{\Delta \in \Delta : \bar{\sigma}(\Delta) \leq 1\}. \tag{11}$$

A permissible  $\Delta$  in  $B\Delta$  destabilizes the system if and only if:

$$\det[I - P(j\omega)\Delta(j\omega)] = 0. \tag{12}$$

A new function called the Structured Singular Value Function (known as  $\mu$ ) is defined as follows:

$$\mu(P(j\omega)) = \begin{cases} \left[ \min_{\Delta \in B\Delta} \bar{\sigma}(\Delta(j\omega)) : \det(I - P\Delta) = 0 \right]^{-1} \\ \text{Otherwise,} \\ 0 \quad \text{if} \quad \det[I - P\Delta] \neq 0 \quad \forall \quad \Delta \in B\Delta \end{cases} \tag{13}$$

where  $\bar{\sigma}$  denotes the maximum singular value (Doyle 1982).

It can be shown that for the feedback system to remain stable for all stable and bounded  $\Delta$ 's,  $\mu$  has to be less than 1 over all frequencies (Karkoub *et al.* 2000):

$$\sup_{\omega} \mu(P(j\omega)) \leq 1. \tag{14}$$

For computation purposes, it was shown by Doyle (1982) that:

$$\rho(P) \leq \mu(P) \leq \bar{\sigma}(P). \tag{15}$$

However, since the difference between the spectral radius,  $\rho$ , and the maximum singular value,  $\bar{\sigma}$ , can be arbitrarily large, better estimates of the lower and upper bounds of  $\mu$  should be obtained.

Let  $\mathbf{D}$  be defined as follows:

$$\mathbf{D} = \left\{ \begin{array}{l} \text{diag}[D_1, \dots, D_s, d_1 I_1, \dots, I_{mF} : \\ D_i \in C^{r_i \times r_i}, D_i = D_i^* > 0 \\ d_j \in \mathbf{R}, d_j > 0 \end{array} \right\} \quad (16)$$

and

$$\mathbf{Q} = \{Q \in \Delta : Q^* Q = I_n\} \quad (17)$$

and let  $D$  be in  $\mathbf{D}$  such that  $D\Delta = \Delta D$ , then,

$$\max_{Q \in \mathbf{Q}} \rho(QP) \leq \max_{\Delta \in B\Delta} \rho(\Delta P) = \mu_\Delta(P) \leq \inf_{D \in \mathbf{D}} \bar{\sigma}(DPD^{-1}). \quad (18)$$

This result has proven to be very important in determining an upper bound for  $\mu$ .

So far, we have derived conditions for the structured and unstructured uncertainty case that have to be met for the feedback system to be robustly stable. However, in practice, one is usually concerned with maintaining stability as well as a good level of performance. Consider the system shown in Fig. 3, and define  $v$  and  $y$  such that the condition  $\|P_{11}\|_\infty$  is less than 1 and becomes the performance specification (Maciejowski 1989):

$$\begin{Bmatrix} y \\ x \end{Bmatrix} = \begin{bmatrix} P_{11} & P_{12} \\ P_{21} & P_{22} \end{bmatrix} \begin{Bmatrix} v \\ z \end{Bmatrix}. \quad (19)$$

So, for robust performance to be achieved,

$$\|P_{11} + P_{12}\Delta(I - P_{22}\Delta)^{-1}P_{21}\|_\infty \leq 1 \quad (20)$$

and

$$\sup_{\omega} \mu(P_{22}(j\omega)) \leq 1. \quad (21)$$

The above two conditions can be further simplified by writing the system's performance requirements as fictitious uncertainty blocks as shown in Fig. 3. The stability uncertainty block  $\Delta$  and the fictitious performance uncertainty block  $\Delta_0$  can be rearranged to look like Fig. 2, leading to a new uncertainty block  $\Delta = \text{diag}(\Delta_0, \Delta)$  and a new plant  $P$ . It was shown by Doyle (1982) that if we are to require:

$$\sup_{\omega} \mu(P) \leq 1 \quad (22)$$

then, Eqs. (20) and (21) are satisfied. Also, it turns out that Eq. (22) is a necessary condition for Eq. (20) to hold. Therefore, in order for us to achieve robust performance, the condition described by Eq. (22) had to be met.

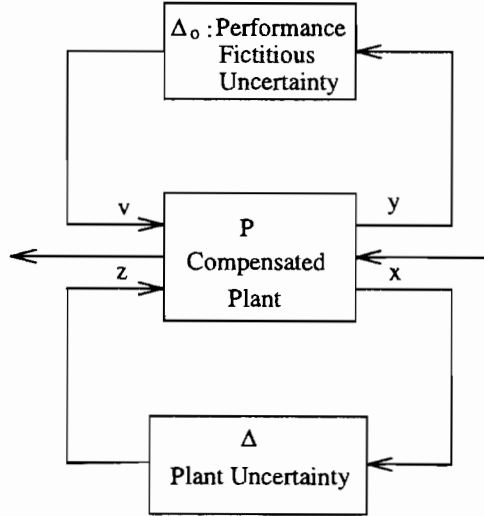


Fig. 3. Block diagram for robust performance.

### D-K iteration

The  $\mu$ -synthesis is adopted in the design of the control law for the double-effect distillation column. This technique is a two-stage synthesis process: the first is designing an  $H_\infty$  controller and the second is using the structured singular value function,  $\mu$ , for synthesis. The  $\mu$  values of the closed-loop can be determined by using scaling matrices and calculating the infinity norm. D-K iteration, which is a minimization scheme, is used to obtain less conceivable bounds on the  $\mu$  values across the frequency spectrum. D-K iteration is basically a two-step minimization process: the first step is a minimization over all stabilizing controllers  $K$  while the scaling matrix  $D$  is held fixed, and the second step is a minimization over  $D$  while  $K$  is kept fixed. The flow chart shown in Fig. 4 summarizes the procedure for D-K iteration (Maciejowski 1989). The symbols used in the flow chart are defined as follows:

$$D_\omega = \text{diag}[d_1^\omega I, d_2^\omega I, \dots, d_f^\omega I, \Delta_1^\omega, \dots, \Delta_F^\omega], \quad (23)$$

$$D(s) = \text{diag}[d_1(s)I, d_2(s)I, \dots, d_r(s)I, D_1(s), \dots, D_F(s)], \quad (24)$$

$$\hat{P}(s) = \begin{bmatrix} D(s) & 0 \\ 0 & I \end{bmatrix} P(s) \begin{bmatrix} D^{-1}(s) & 0 \\ 0 & I \end{bmatrix} = \begin{bmatrix} \hat{P}_{11}(s) & \hat{P}_{12}(s) \\ \hat{P}_{21}(s) & \hat{P}_{22}(s) \end{bmatrix}, \quad (25)$$

$$P_{cl} = \hat{P}_{11} + \hat{P}_{12}K(I - \hat{P}_{22}K)^{-1}\hat{P}_{21}, \quad \text{and} \quad (26)$$

$$\hat{P}_{cl} = D_\omega \hat{P}_{cl} D_\omega^{-1}. \quad (27)$$

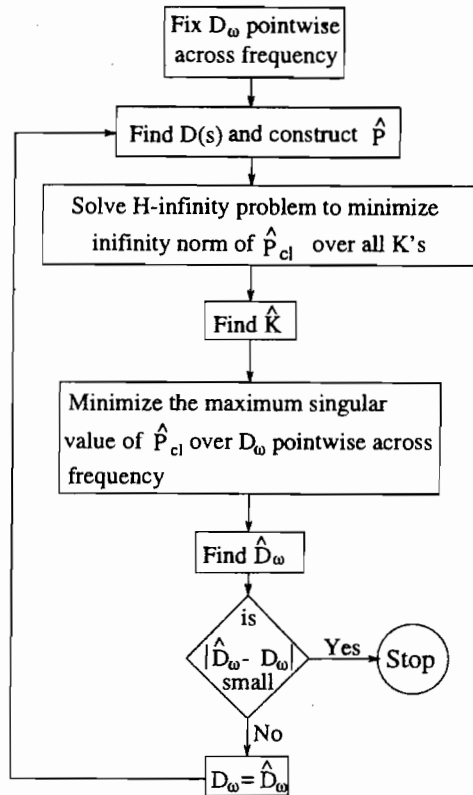


**Fig. 4.** Block diagram for D–K iteration.

**Remark.** The D–K iteration procedure calculates the upper and lower bounds of the  $\mu$ -function across all frequencies. If the difference between the upper and lower bounds is large, the iteration weights are changed until convergence between the bounds occurs. If the bounds are close to each other and the maximum value of the  $\mu$ -function is still larger than 1, then the performance requirements have to be relaxed to achieve robust performance. It is worth mentioning that convergence of the D–K iteration is related to the convexity of the closed-loop system, which is difficult to prove *a priori*.

### $\mu$ -Synthesis versus PI control

As was mentioned earlier, several researchers prefer to use PI control when it comes to distillation columns. PI control is easy to apply and the controllers can be made workable by using tuning techniques such as biggest modulus turning (BMT). However, this method has several drawbacks: (1) the controllers are assumed to be independent, i.e., no loop affects the other; this is true only under very special circumstances. The other problem that arises from this assumption is which input to pair with which output. Most of the work available in the literature is done in an ad-hoc manner and no guarantees are given for stability for robustness



(Skogestad & Morari 1988, Al-Elg & Palazoglu 1989). (2) This control design technique assumes that the model is exact; however, it has been shown that the accuracy of the model depends on several assumptions such as efficiency, pressure, and number of trays. These problems are taken care of when using the  $\mu$ -synthesis technique. It is assumed that the control design model has some errors associated with it due to the assumptions made while deriving the model and the uncertainties associated with the parameters. Moreover, the controller does not have to be diagonal which allows interaction between the various control loops.

### **$\mu$ -Synthesis versus IBC**

Inverse based controllers (IBC) have been used by several authors including Skogestad and Morari (1988) and Pohlmeier and Rix (1996) for the control of distillation columns. It was shown that this method performs better than the PI procedure. The problem with this method is that the procedure is ad-hoc (as is the PI method) and involves a great deal of trial and error. The work done by Pohlmeier and Rix (1996) assumes that the plant has a specified multiplicative uncertainty and neglected parameter, input, and actuation uncertainties, and noise. Even then, the authors had to go through a lengthy procedure to tune the controllers.

In the  $\mu$ -synthesis procedure, a mutual balance between robustness and performance is achieved. All reasonable uncertainties can be inserted in the control design model (Doyle 1982) and the final controller is guaranteed to be robust by assuring that the  $\mu$  values are less than 1 for all frequencies.

### **$\mu$ -SYNTHESIS CONTROLLER DESIGN**

A schematic diagram of the double-effect distillation column is shown in Fig. 5. Most linear dynamic models available in the literature do not represent the double-effect distillation column with high fidelity, especially at high frequencies. Hence, the control design needs to account for these discrepancies. The neglected high frequency dynamics as well as unmodeled phenomena are accounted for in the  $\mu$ -synthesis control design procedure using an additive uncertainty function. This function has the following feature: low magnitude at low frequencies and high magnitude at high frequency (see Fig. 6). The shape of the additive uncertainty weight indicates that the system has a low margin of error at low frequency and high margin of error at high frequencies. Therefore, the controller needs to roll off at the crossover frequency of the uncertainty weight.

One other problem to be addressed is the actuation error. This could be troublesome if the actuator is highly nonlinear. To account for the actuation and input uncertainty, a multiplicative input weighting function is included in the control design model. This represents a low margin of error in the actuator model at low frequencies (5%) and a relatively larger margin of error at high frequencies (see Fig. 6). It is worth mentioning that the control design should force the controller to roll off before the actuation error becomes significant. Moreover, the controller should satisfy pre-specified performance criteria for the response of the distillate as well as the bottoms. These performance criteria are inscribed in the performance weights “W\_perf\_b1”, “W\_perf\_d1”, “W\_perf\_b2”, and “W\_perf\_d2” (see Figs. 6 and 7).

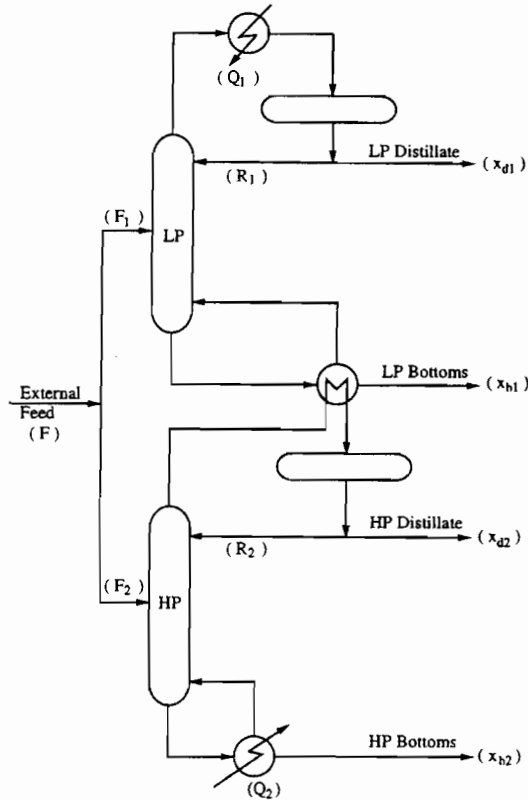


Fig. 5. Schematic diagram of a double-effect distillation column.

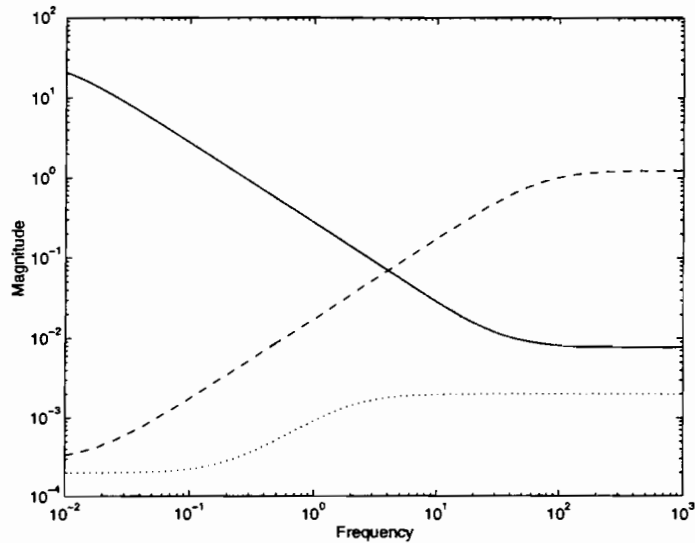


Fig. 6. Uncertainty magnitude plots. Performance weight (solid), additive uncertainty (dashed), and actuation uncertainty (dotted).

### $\mu$ -Synthesis control structure

The block diagram shown in Fig. 7 describes the control system used in this work. The block “double-effect column” contains the transfer matrix given by Eq. (1). Since the errors in the model increase with frequency due to the unmodeled high frequency dynamics, additive uncertainty described by the block “w\_add1” through “w\_add4” is added to the outputs of the system.

Implementation of the controller requires sensor measurements of certain quantities in the distillation process. Therefore, noise can also be a factor in the overall dynamics of the double-effect distillation column. To account for this effect a fictitious sensor noise is included in the dynamic model. The block “sens\_nois” is a constant transfer function representing the noise that can be incurred during the implementation of the controller.

The command input to the double-effect distillation column is usually transmitted through a device/actuator. Therefore, the model of the actuator might have some errors associated with it. Hence, the control design model has to account for these errors to avoid unexpected behavior. In this control design, the actuation as well as the input uncertainties are accounted for using the blocks “w\_act1” through “w\_act4”.

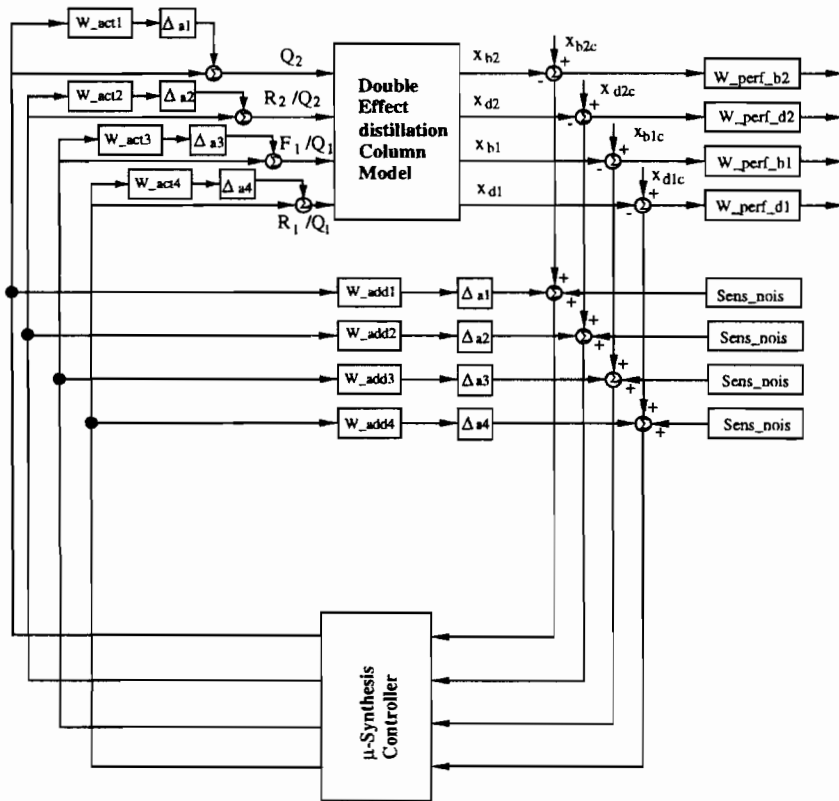


Fig. 7. Block diagram for the  $\mu$ -synthesis control design.

### Controller design

Two controllers have been designed for a double-effect distillation column using the  $\mu$ -synthesis technique. The control design model is different for both controllers. The first controller is designed based on a transfer matrix that did not consider the time delays of the system. Since the additive uncertainty used in the design process assumes that there is error in the system, the time delays can be considered an error. The uncertainty is represented by a disk around the transfer matrix at every frequency. This means that the phase error at any frequency can be arbitrarily large. The second designed controller is similar to the first one; however, the transfer matrix includes the time delays. Since the  $\mu$ -synthesis technique assumes a linear transfer matrix, the time delays are linearized. The linearization is performed using the second order Pade approximation. There are several techniques for linearizing a transport delay; however, the Pade method is most suited for this kind of problem. The Pade approximation for a typical time lag  $e^{-T_d s}$  is given by:

$$e^{-T_d s} \simeq \frac{1 - \frac{T_d}{2}s + \frac{(T_d s)^2}{12}}{1 + \frac{T_d}{2}s + \frac{(T_d s)^2}{12}} \quad (28)$$

The expression given by Eq. (28) is used to linearize the transport lags in the transfer matrix for the double-effect distillation column given by Eq. (1). The cutoff frequency of the linearized transport lag occurs after the corner frequency of the transfer function. This reduces the risk of having performance limitations due to the presence of the right half zeros of the linearized transport lag.

### RESULTS

One aspect of  $H_\infty$  control design is that it allows the designer to introduce quantitative errors into the model. The additive uncertainty assumes that at each frequency there is a disk of errors whose radius is pre-specified. Therefore, additive uncertainty can be used to compensate for phase discrepancies. Knowing that transport lag introduces a phase shift in a narrow frequency region, additive uncertainty can be used to compensate for the effect of these lags. Based on this theory, a controller was designed with no regard to the transport lags. The  $\mu$ -synthesis controller performed relatively well when simulated with the non-lagged transfer matrix. However, when simulated with the actual transfer matrix, the controller led to a lower-than-average performance (see Fig. 8 through 11). Although the controller was robust and showed smooth behavior when compared to the PI controller, the overall behavior of the system was unacceptable. Therefore, a different approach had to be followed.

A second controller was designed in a similar manner to the first one except the transfer matrix contained linearized transport lags, using the Pade approximation. The controller was tested for robustness using corrupted signals and adequately constructed disturbances. The response time was better than the first  $\mu$ -synthesis controller as well as the PI controller (see Fig. 12 through 15). The LP as well as the HP bottoms and distillates did not oscillate as much as in the PI controller case. The bottoms and distillates reached the target in a smooth manner without

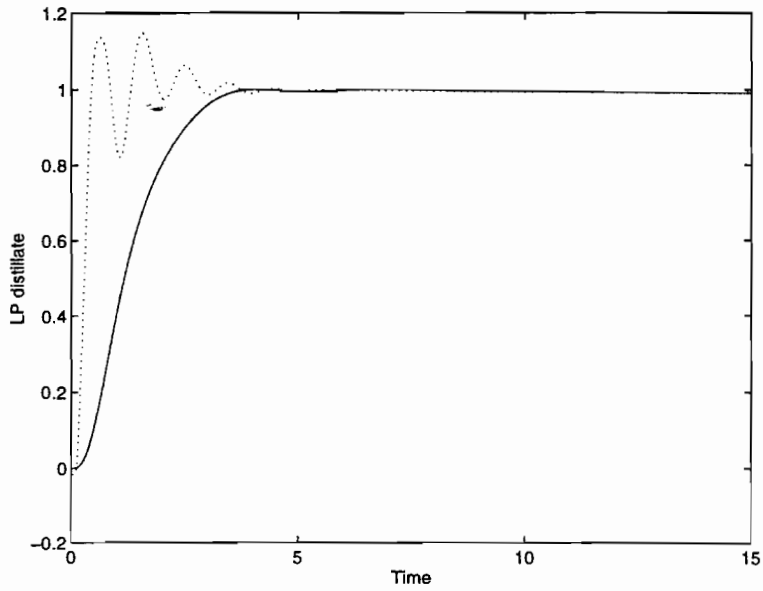


**Fig. 8.** Comparison between the LP distillate response using a  $\mu$ -synthesis controller for a transfer matrix with zero lag (solid) and a PI controller (dotted).

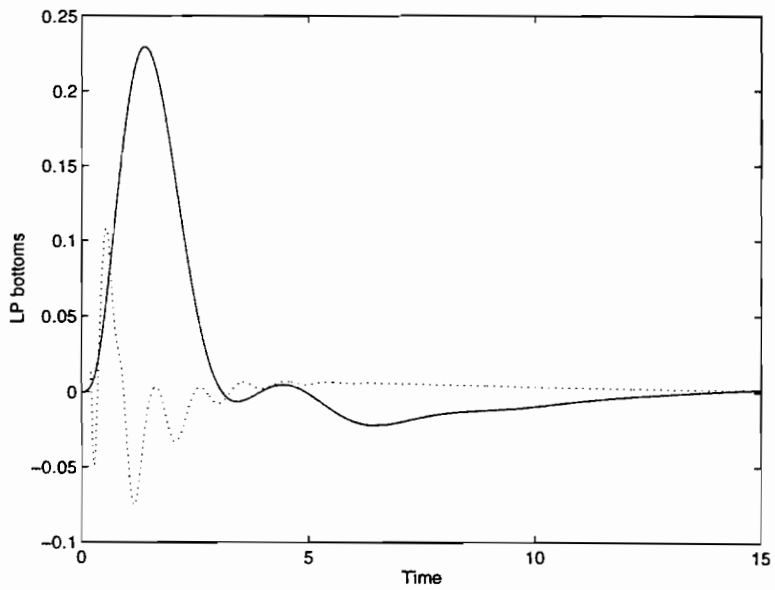


**Fig. 9.** Comparison between the LP bottoms response using a  $\mu$ -synthesis controller for a transfer matrix with zero lag (solid) and a PI controller (dotted).

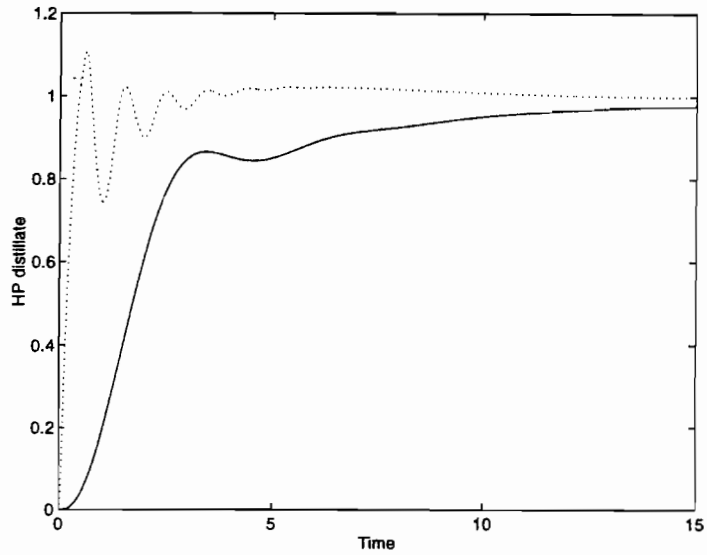


**Fig. 10.** Comparison between the HP distillate response using a  $\mu$ -synthesis controller for a transfer matrix with zero lag (solid) and a PI controller (dotted).

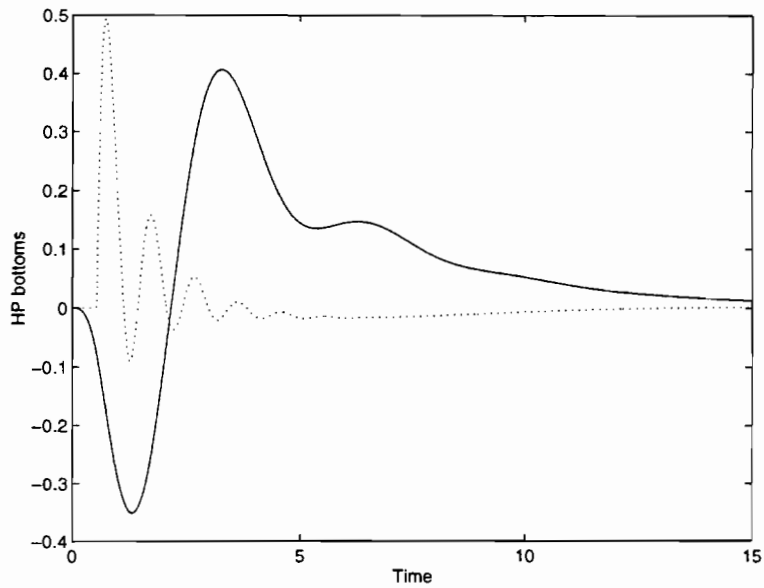


**Fig. 11.** Comparison between the HP bottoms response using a  $\mu$ -synthesis controller for a transfer matrix with zero lag (solid) and a PI controller (dotted).

overshooting (see Fig. 12 through 15). This controller was also robust to variations in high frequency dynamics, actuation uncertainty, input uncertainty, and noise. The controller was simulated with the actual transfer matrix and the results were excellent.

The maximum value for the LP bottoms was a little higher with the  $\mu$ -synthesis controller than with the PI controller (see Fig. 15). However, the settling time was slightly shorter with the  $\mu$ -synthesis controller. If the performance requirements were to be relaxed for the LP bottoms, the maximum value would be reduced; however, the settling time would increase. Table 1 compares the settling times and the maximum values of the LP and HP distillates as well as the LP and HP bottoms. It is clear that the  $\mu$ -synthesis controller leads to good performance results.

### CONCLUDING REMARKS

Two  $\mu$ -synthesis controllers were designed for a double-effect distillation column. The first controller was designed with no regard to the inherent transport lags of the system. This controller did not perform well, which indicated that the time delays in the system were larger than what it was represented by in the various uncertainty models. A second controller was designed using the  $\mu$ -synthesis and the Pade approximation for the transport lags. The results were excellent. The  $\mu$ -synthesis controller outperformed the PI controller as well as the first  $\mu$ -synthesis controller.

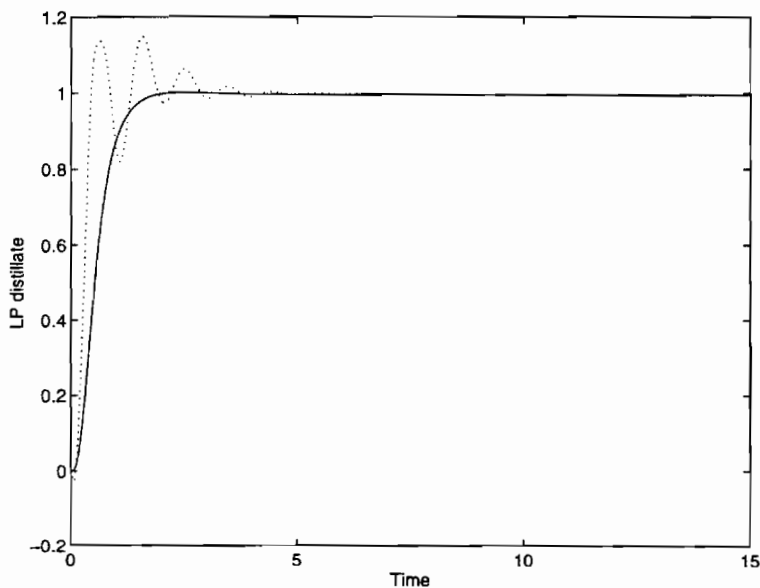


**Fig. 12.** Comparison between the LP distillate response using a  $\mu$ -synthesis controller for a lagged transfer matrix (solid) and a PI controller (dotted).

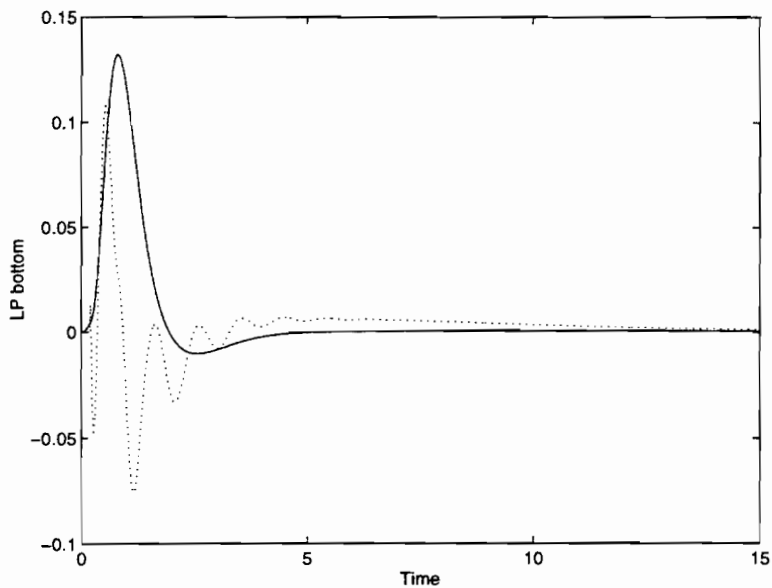


**Fig. 13.** Comparison between the LP bottoms response using a  $\mu$ -synthesis controller for a lagged transfer matrix (solid) and a PI controller (dotted).

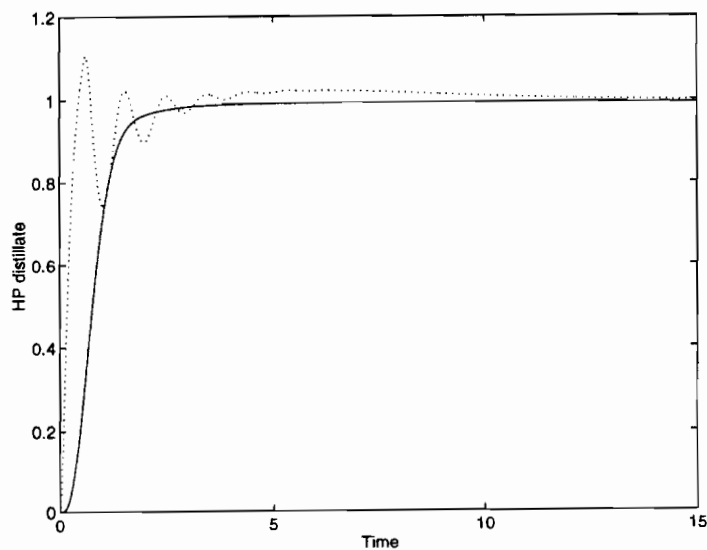


**Fig. 14.** Comparison between the HP distillate response using a  $\mu$ -synthesis controller for a lagged transfer matrix (solid) and a PI controller (dotted).



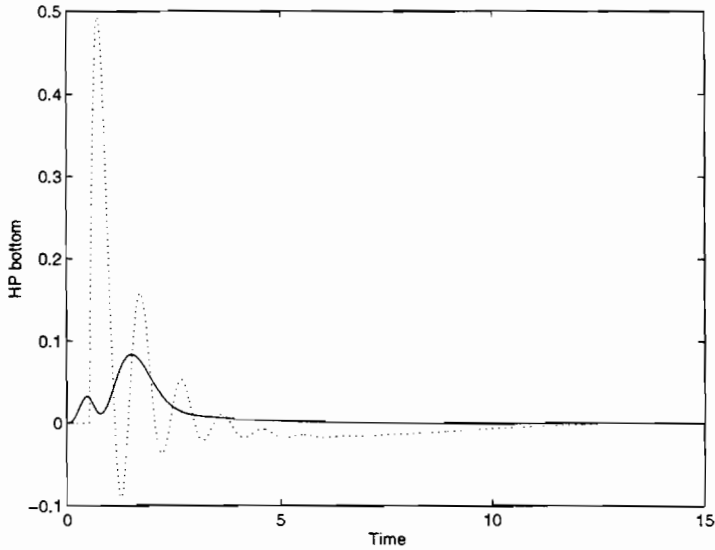


**Fig. 15.** Comparison between the HP bottoms response using a  $\mu$ -synthesis controller for a lagged transfer matrix (solid) and a PI controller (dotted).

**Table 1.** Performance data for the  $\mu$ -synthesis controller without lags,  $\mu$ -synthesis controller with lags, and PI controller.

		$\mu$ -synthesis (no lag)	$\mu$ -synthesis (with lag)	PI
LP Distillate	Settling Time	3.5 s	2 s	4 s
	Max. Value	1.05	1.02	1.175
LP Bottoms	Settling Time	14 s	4 s	5 s
	Max. Value	0.225	0.125	0.11
HP Distillate	Settling Time	14 s	2 s	5 s
	Max. Value	–	1.0	1.15
HP Bottoms	Settling Time	14 s	3.5 s	5 s
	Max. Value	0.4	0.08	0.5

### ACKNOWLEDGEMENT

The author would like to thank Kuwait University for supporting this project.

### REFERENCES

- Al-Elg, A.H. & Palazoglu, A. 1989.** Modeling and control of a high purity double effect distillation column. *Computers and Chemical Engineering* **13(10)**: 1183–1187.
- Balas, G., Doyle, J., Glover, K., Packard, A. & Smith, R. 1991.**  $\mu$  Analysis and Synthesis Toolbox. MUSYN and The Mathworks Inc., Natick, MA, USA.
- Doyle, J. 1982.** Analysis of feedback systems with structured uncertainties. *Proceedings of the Institute of Electrical Engineers, Part D* **129**: 242–250.

- Han, M. & Park, S. 1996.** Multivariable control of double-effect distillation configurations. *Journal of Process Control* **6(4)**: 247–253.
- Karkoub, M., Balas, G., Tamma, K. & Donath, M. 2000.** Modeling and robust control of single-link robot arms. *Control Engineering Practice* **8(7)**: 725–734.
- Lee, J.H. & Morari, M. 1990.** Robust control structure selection and control system design methods applied to distillation column control. *Proceedings of the 29th Conference on Decision and Control*, Honolulu, Hawaii, USA.
- Maciejowski, J.M. 1989.** *Multivariable Feedback Design*. Addison-Wesley Publishers Ltd., London, UK.
- Pohlmeier, J. & Rix, A. 1996.** Interactive plant and control design of a double-effect distillation column. *Computers and Chemical Engineering* **20(4)**: 395–400.
- Skogestad, S. & Morari, M. 1988.** LV-control of a high purity distillation column. *Chemical Engineering Science* **43(1)**: 33–48.

*(Submitted 31 July 2000)*

*(Revised 9 January 2001)*

*(Accepted 20 January 2001)*

## طريقة $\mu$ للتحكم الفعال لأعمدة التقطير الازدواجية

منصور كركوب

قسم الهندسة الميكانيكية

كلية الهندسة والبتروول - جامعة الكويت

### الخلاصة

يعتبر التحكم لأعمدة التقطير الازدواجية مجال خصب لكثير من الباحثين في السنوات القليلة الماضية. ولقد كانت الطريقة التكاملية والتناسبية معا (PI) هي أداة التحكم المفضلة التي استعملت مع أعمدة التقطير علي الرغم من أن هذه الطريقة تتطلب نموذج على درجة عالية من الدقة ولا تضمن أداء فعال عند استعمال النموذج بشكل عام بالإضافة إلى الأخطاء الأخرى التي تنتج عن ذلك. لذا استلزم الأمر تصميم طريقة تحكم أخرى للتغلب على عيوب النموذج الديناميكي. ولقد أثبتت طريقة  $\mu$  فعاليتها لراب الصدع بين المحاكاة وعمليات التحكم الخاصة بالتصميم. وقد تم خلال هذا البحث تصميم وحدتان للتحكم لأعمدة التقطير الازدواجية باستعمال طريقة  $\mu$  للتحكم الخاص بالتصميم.

والوحدتان اللتان تم تصميمهما تم استنتاجها من النموذج الذي اشتق بواسطة ألاج وبالازجلو عام 1989. هذا وقد أدت النتائج المستخلصة إلى حدوث تجاوب أفضل بالنسبة لوحدي الضغط العالي والضغط المنخفض معا وكذلك لقاءات كلا من الوحدتين. أضف إلى ذلك أن وحدات التحكم التي تم تصميمها قد أثبتت فعاليتها بالنسبة إلى المتغيرات الديناميكية ذات التردد العالي والتشغيل وكذلك المدخلات المشكوك فيها والضوضاء بصفة عامه.

الكلمات الإفتاحية:-

أعمدة التقطير الإزدواجية- طريقة  $\mu$ - التحكم الفعال.

